2026 IEEE/SICE International Symposium on System Integration (SII)
January 11-14, 2026. Cancún, México

A Teleoperation Framework for an Articulated Aerial Robot with Full DoF Mapping of Base Pose and Joint Angles

Kotaro Kaneko[1,2], Junichiro Sugihara[1], Kazuki Sugihara[3], Masaki Kitagawa[1], Keisuke Nagato[2], and Moju Zhao[1]

***Abstract*— Robots are increasingly being used to replace humans in performing dangerous tasks, and aerial robots are particularly popular for work at heights. Both underactuated and fully actuated multirotors have mainly been used, but the range of tasks they can perform is limited due to their low degree of operational freedom. Articulated aerial robots are attracting attention as one solution to this problem. Due to the complexity and numerous disturbances involved in high-altitude work, teleoperation by humans is still necessary, and research is ongoing. Most of these studies focus on conventional multi-rotors, and it is difficult to intuitively control articulated aerial robots. Therefore, in this study, we propose a new teleoperation framework that allows operators to intuitively control all degrees of freedom of an articulated aerial robot simultaneously. The proposed framework consists of a floating-based device that acquires operating inputs by utilizing the freedom of movement of both human hands, and a system that generates commands to the robot from those inputs. The effectiveness of the proposed framework was verified through operating experiments using a real robot and wall cleaning task.**

I. INTRODUCTION

In recent years, robots have been increasingly used to replace humans in dangerous work environments. High-altitude work in particular requires urgent replacement due to the high risk of injury to workers, and aerial robots are mainly used for this purpose. Although it is possible to perform work at high altitudes with a conventional robot arm, additional equipment such as a gondola is required to lift it to a high altitude, which limits their usability in various locations. In contrast, aerial robots applied in diverse environments because they have the ability to access high altitudes on their own.

In conventional robot-based high-altitude work, under-actuated quadrotors have been mainly used [1–3]. While these robots are suitable for work due to their hovering capability, they only have four DoF (degrees of freedom): three translational DoF and one rotational DoF in the yaw direction. This limited DoF restricts the variety of tasks they can perform. In order to expand the range of tasks that can be performed, it has been proposed to use fully actuated multi-rotors with an increased number of rotors or a mechanism for changing the direction of rotors [4–6], but this only increases the DoF in the roll and pitch directions, which is not sufficient for complex tasks. As a method of increasing DoF of robot maneuverability, articulated aerial robots are proposed [7–9]. These robots have joints in their bodies, which increases their DoF and allows them to perform tasks that were not possible with conventional multi-rotors.

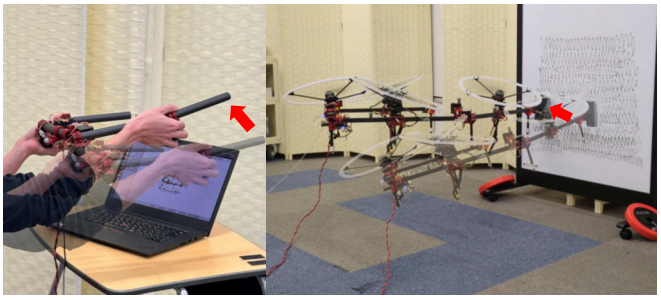

Fig. 1: A human operator is teleoperating an articulated aerial robot by using both hands. By using our proposed framework, the operator can intuitively teleoperate all DoF of the robot simultaneously.

In replacing high-altitude work with robots, it is ideal for robots to perform tasks completely autonomously, and research on autonomous control has also made remarkable progress [10]. However, due to the complexity and numerous disturbances in high-altitude work environments, the need for human operators remains significant [11]. By utilizing human's ability to make appropriate judgments, it is possible to perform optimal operations in real time even in unknown environments or with unknown work objects. This requires a teleoperation framework that allows intuitive and easy control of the robot. Many teleoperation frameworks for aerial robots have been proposed [12–15]. Most of these operate targets are conventional multi-rotors. Even if these methods are used as they are for operating articulated aerial robots, it is difficult to intuitively control all DoF of the robot, especially its joints. In order to fully utilize the advantages of articulated aerial robots, a new teleoperation framework is necessary.

In this study, we propose a teleoperation framework for utilizing multi-jointed aerial robots in high-altitude work as shown in Fig. 1. An overview of the proposed framework is shown in Fig. 2. The contributions of this study are as follows.

- We propose a new teleoperation device that allows

[1]DRAGON Lab, Department of Mechanical Engineering, The University of Tokyo, Tokyo 113-8656, Japan {chou, j-sugihara, kitagawa}@dragon.t.u-tokyo.ac.jp
[2]HNL Lab, Department of Mechanical Engineering, The University of Tokyo, Tokyo 113-8656, Japan {kaneko, nagato}@hnl.t.u-tokyo.ac.jp
[3]JSK Lab, Department of Mechano-Informatics, The University of Tokyo, Tokyo 113-8656, Japan sugihara@jsk.imi.i.u-tokyo.ac.jp

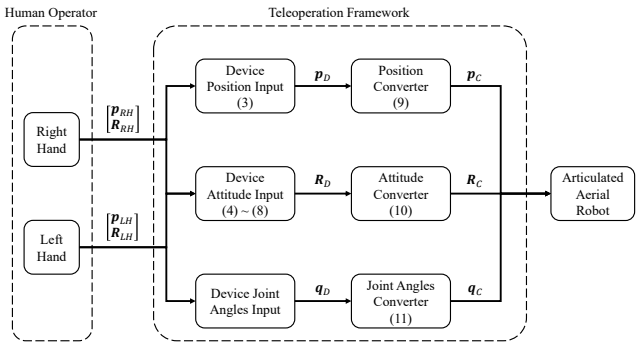

Fig. 2: System diagram of proposed teleoperation framework. $\boldsymbol{p}_{RH}$ and $\boldsymbol{R}_{RH}$ are the position and rotation of the operator's right hand, $\boldsymbol{p}_{LH}$ and $\boldsymbol{R}_{LH}$ are the position and rotation of the left hand. $\boldsymbol{p}_D$, $\boldsymbol{R}_D$, and $\boldsymbol{q}_D$ are the position, rotation, and joint angles of the proposed device. $\boldsymbol{p}_C$, $\boldsymbol{R}_C$, and $\boldsymbol{q}_C$ are the target position, target rotation, and target joint angles of an articulated aerial robot.

intuitive operation of all DoF of articulated aerial robots.

- We propose a teleoperation system for outputting operation commands corresponding to the proposed device input.
- We demonstrate the effectiveness of the proposed framework through teleoperation experiments using a real robot and wall cleaning tasks.

II. TELEOPERATION DEVICE

This chapter describes a device that allows operator to intuitively input commands corresponding to all DoF of an articulated aerial robot.

A. Degrees of Freedom of an Articulated Aerial Robots

The articulated aerial robots targeted for operation in this study have a skeleton with multiple links connected by rotating joints. The DoF per joint is different depending on the robot, but the maximum is two DoF in the pitch and yaw directions, as shown in the left side of Fig. 3. The DoF in the roll direction is not considered as an operation target because it does not change the overall shape of the robot. In addition, the robot as a whole has three DoF in translation and three DoF in rotation, as shown in the right side of Fig. 3. Therefore, the operatable DoF of an articulated aerial robot d_{robot} can be expressed as follows:

$$d_{\text{robot}} = (n-1) \times 2 + 6, \tag{1}$$

where n is the number of links of the robot. In this study, we aim to operate all of these DoF simultaneously.

B. Required Device Functions

When humans operate a robot, they generally use both hands. In the case of teleoperation for underactuated multi-rotor, a device that has two sticks operated by the fingers of both hands, such as a joystick, is frequently used. Since each stick can move in two directions, a total of four DoF can

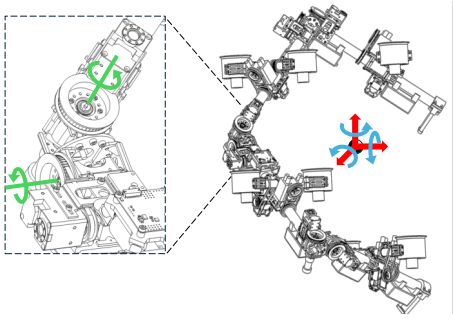

Fig. 3: Image of the teleoperation target articulated aerial robot. Left: DoF of each joint (pitch and yaw rotation). Right: DoF of whole body (translation and rotation).

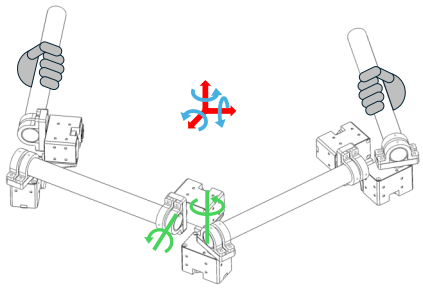

Fig. 4: Design of proposed device for operating articulated aerial robot. The operator uses this device by holding both ends of the link with both hands.

be operated. In the case of teleoperation for fully actuated multi-rotor, a method such as the method in [16] is used, which considers one hand as a single rigid body and inputs its position and attitude. This allows for control of the six DoF (translation and rotation) inherent to the rigid body. As mentioned in the previous section, the articulated aerial robot to be operated in this study has more than six DoF, so neither of these methods is sufficient. Therefore, we propose a method that uses a total of 12 DoF as input by considering both hands as two rigid bodies. Using this method, the following relationship between d_{robot} and human hand's DoF is formed:

$$\begin{aligned} d_{\text{robot}} &= (n-1) \times 2 + 6 < 6 \times 2, \\ n_{\max} &= 4, \end{aligned} \tag{2}$$

where $n_{\max}$ is the maximum number of links that can operate. Therefore, the proposed method can operate articulated aerial robots with up to four links.

C. Design of Device

We designed a device as shown in Fig. 4. Based on the discussion in the previous sections, the target of operation is an articulated aerial robot with four links and two degrees of rotational freedom at each joint, and the device has a similar skeleton structure. This allows the operator to immediately understand what kind of joint angle command is being sent. In addition, by making the device a floating-based device that can be lifted with both hands, it is possible to receive

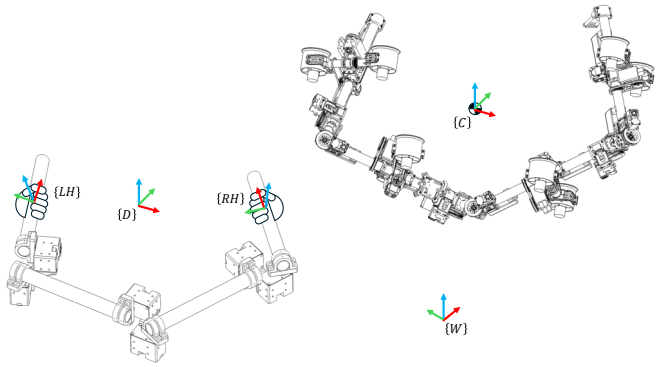

Fig. 5: Image of coordinate systems. $\{RH\}$ is the right hand's coordinate. $\{LH\}$ is the left hand's coordinate. $\{D\}$ is the device's coordinate. $\{C\}$ is the robot's coordinate.

all 12 DoF of both hands as input. The operator uses the device by holding the links at both ends of the device.

III. TELEOPERATION SYSTEM

This chapter describes the system for sending control commands when using the new teleoperation device proposed in the previous section. This system uses the position and attitude of both hands as input to command the position, attitude, and joint angle commands for the articulated aerial robot.

A. Notation and Coordinate System

In this section, we denote scalars in unbold $x, X \in \mathbb{R}$, vectors in bold lowercase $\boldsymbol{x} \in \mathbb{R}^n$, and matrix in bold uppercase $\boldsymbol{X} \in \mathbb{R}^{n\times m}$. We define the coordinate system of operator's right hand as $\{RH\}$, left hand as $\{LH\}$, the device as $\{D\}$, the robot CoG as $\{C\}$, and world as $\{W\}$ as shown in Fig. 5. And we denote the position vector of the origin of $\{A\}$ in the $\{W\}$ as $\boldsymbol{p}_{\{A\}}$, and rotational matrix from $\{W\}$ to $\{A\}$ as $\boldsymbol{R}_{\{A\}}$.

B. Input from Operator's Hands to Device

1) Position: The device position $\boldsymbol{p}_D$ is calculated from the position of the operator's right hand $\boldsymbol{p}_{RH}$ and the position of the left hand $\boldsymbol{p}_{\mathrm{LH}}$ as follows:

$$\boldsymbol{p}_{\{D\}} = \frac{(\boldsymbol{p}_{\{RH\}} + \boldsymbol{p}_{\{LH\}})}{2}. \tag{3}$$

2) Attitude: Rotational matrix $\boldsymbol{R}_{\{D\}}$ is described as follow:

$$\boldsymbol{R}_{\{D\}} = (\boldsymbol{x}_D, \boldsymbol{y}_D, \boldsymbol{z}_D), \tag{4}$$

where each vectors are basis vectors. The basis vectors of $\boldsymbol{R}_{\{D\}}$ are calculated from the basis vectors of $\boldsymbol{R}_{\{RH\}}$ and $\boldsymbol{R}_{\{LH\}}$ as follows:

$$\boldsymbol{x}_D = \frac{\boldsymbol{x}_{RH} + \boldsymbol{x}_{LH}}{\|\boldsymbol{x}_{RH} + \boldsymbol{x}_{LH}\|}, \tag{5}$$

$$\boldsymbol{y}_D^{'} = \frac{\boldsymbol{y}_{RH} + \boldsymbol{y}_{LH}}{\|\boldsymbol{y}_{RH} + \boldsymbol{y}_{LH}\|}, \tag{6}$$

$$\boldsymbol{y}_D = \frac{\boldsymbol{y}_D^{'} - (\boldsymbol{y}_D^{'} \cdot \boldsymbol{x}_D)\boldsymbol{x}_D}{\|\boldsymbol{y}_D^{'} - (\boldsymbol{y}_D^{'} \cdot \boldsymbol{x}_D)\boldsymbol{x}_D\|}, \tag{7}$$

$$\boldsymbol{z}_D = \boldsymbol{x}_D \times \boldsymbol{y}_D. \tag{8}$$

Generating the basis vector of the $\boldsymbol{R}_{\{D\}}$ in this way means taking the midpoint between the operator's right and left hand rotations.

3) Joint Angles: As mentioned in Sec. II, the DoF of both hands is equal to or larger than that of a robot. Therefore, by solving the inverse kinematics, all joint angles of the device must be determined. Since the device proposed in this study has a skeleton structure similar to that of a robot, the joint state can be physically determined without calculating the inverse kinematics. $\boldsymbol{q}_D$ can be obtained by measuring the angles of each joint of the device.

4) Independence of Input Degrees of Freedom: In this system, the device's position and orientation are determined from the average position and orientation of both hands, and the joint angles of the device are mechanically determined from the relative position and orientation between the two hands. For the 12 DoF from both hands to correspond to the device's 12 DoF, the device's kinematic Jacobian must be regular, meaning the device must not be at a singular mechanical point. In configurations where both ends are aligned in a straight line or in a state of perfect parallelism, the rank of the Jacobian decreases, leading to a loss of independence. Except for singular configurations, the 12 DoF input from both hands can be received independently.

C. Conversion from Input to Command

1) Position Conversion: The robot's target position $\boldsymbol{p}_C(t)$ is generated from the device's position input $\boldsymbol{p}_D(t)$ as follows:

$$\boldsymbol{p}_C(t) = \boldsymbol{p}_C(t_0) + \boldsymbol{k}_p \odot (\boldsymbol{p}_D(t) - \boldsymbol{p}_D(t_0)), \tag{9}$$

where t_0 refers to the moment of starting teleoperation, and $\odot$ is the Hadamard product, which is the product of each element of the vector. By commanding the amount of movement from the initial position of the device as the target movement amount of the robot, it is possible to freely determine the position from which the operator begins operation. $\boldsymbol{k}_p$ is the scaling parameter of the movement amount, and there is a trade-off between ease of long-distance movement and ease of precise operation. The operator needs to adjust this parameter appropriately according to the situation.

2) Attitude Conversion: The robot's target rotational matrix $\boldsymbol{R}_{\{C\}}(t)$ is generated from the device's rotational matrix input $\boldsymbol{R}_{\{D\}}(t)$ as follows:

$$\boldsymbol{R}_{\{C\}}(t) = \boldsymbol{R}_{\{D\}}(t). \tag{10}$$

Unlike position commands, by making the input and target attitudes the same, we aim to make it easier for the operator to recognize what attitude commands are appropriate to input. In addition, when operating an underactuated aerial robot, since the robot cannot independently control x and roll, and y and pitch, only target yaw is commanded among the generated target attitudes.

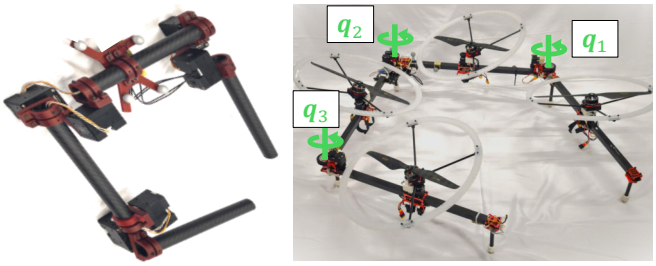

Fig. 6: Left: Snapshot of the teleoperation device. Motion capture markers are attached to measure position and attitude. Servo motors are attached to each joint to measure roll and pitch joint angles. Right: Snapshot of HYDRUS_XI, the articulated aerial robot to be teleoperated. It has three joints (q_1, q_2, q_3) that rotate in the yaw direction.

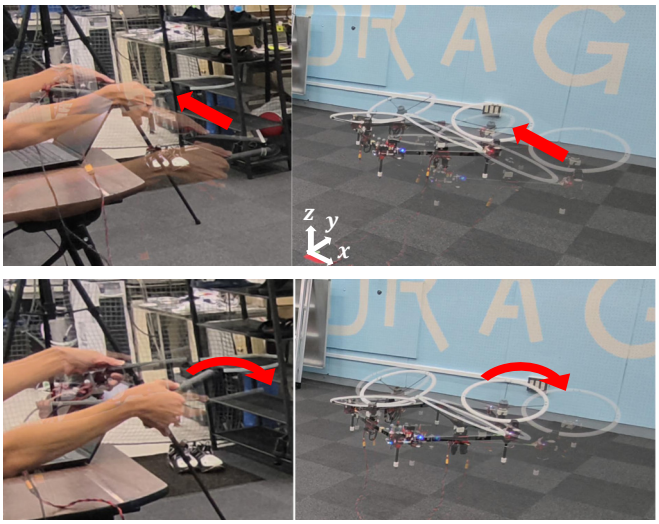

Fig. 7: Snapshots showing the operator performing teleoperation under direct line of sight conditions. Top: The operator moved the device to $-x$ direction, and then the robot moved to same direction. Bottom: The operator moved the device's joint, and then the same joint of the robot moved.

3) Joint Angles Conversion: Similar to attitude commands, by making the input and target joint angles the same, we aim to make it easier for the operator to recognize. In addition, since the range of joint angles that the device can take and the range of joint angles that the robot can take are not always the same, we convert the commands so that they fit within the robot's feasibility range of joint angles. Therefore the robot's target joint angles $\boldsymbol{q}_C(t)$ are generated from the device's joint angle input $\boldsymbol{q}_D(t)$ as follows:

$$q_{C,i}(t) = \begin{cases} q_{\min,i} & \text{if } q_{D,i}(t) < q_{\min,i} \\ q_{D,i}(t) & \text{if } q_{\min,i} \leq q_{D,i}(t) \leq q_{\max,i} \\ q_{\max,i} & \text{if } q_{D,i}(t) > q_{\max,i} \end{cases}, \quad (11)$$

where $q_{C,i}(t)$ and $q_{D,i}(t)$ are the i-th elements of $\boldsymbol{q}_C(t)$ and $\boldsymbol{q}_D(t)$, and $q_{\min,i}$ and $q_{\max,i}$ are the minimum and maximum values of the angles that are feasible for the i-th joint of the robot. If the robot's joint angle has less than two DoF, there are no commands for joints that do not correspond to the robot.

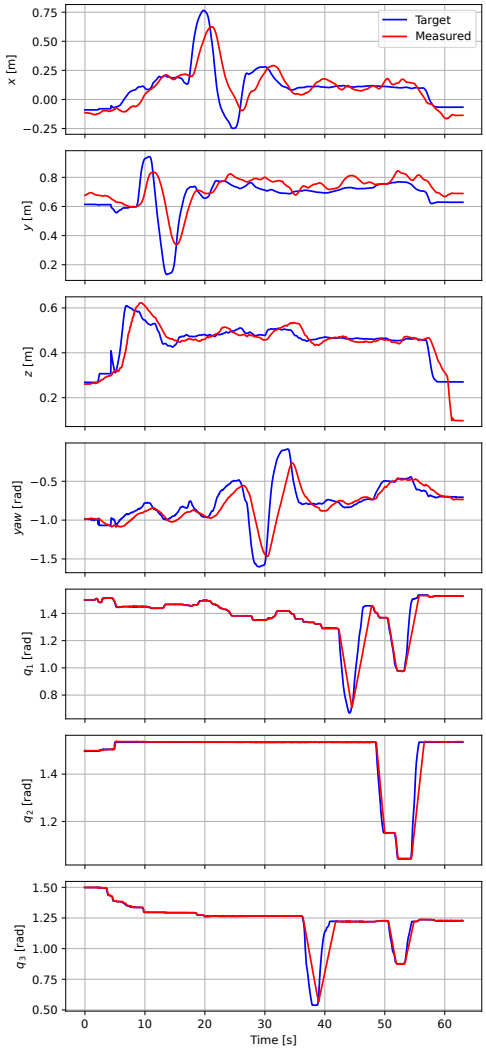

Fig. 8: Results for the teleoperation experiment. The blue line is the target values which commanded from teleoperation system. The red line is the measured values. Position and attitude were measured by Motion Capture system, and joint angles were measured by servo motors of the robot.

IV. EXPERIMENT

A. Setup

The left side of Fig. 6 shows the teleoperation device constructed as described in Sec. II-C. To achieve ease of holding and operating with both hands, each link consists of a carbon pipe with a length of $0.2\,\mathrm{m}$ and a diameter of $0.02\,\mathrm{m}$. Additionally, each link is connected by two servo motors. The values measured by these servo motors are acquired as input for the joint angles described in Sec. III-B. In addition, the use of servo motors makes it possible to lock joints that are not responding when operating a robot with low joint freedom, making operation easier. In order to obtain the

TABLE I: RMSE and delay between target and measured values for position and attitude.

	x	y	z	yaw
RMSE	0.126 m	0.106 m	0.051 m	0.196 rad
Delay	1.253 s	1.303 s	0.652 s	1.303 s

TABLE II: RMSE and delay between target and measured values for joint angles.

	q_1	q_2	q_3
RMSE	0.062 rad	0.029 rad	0.067 rad
Delay	0.500 s	0.375 s	0.525 s

position and attitude inputs described in Sec. III-B, Optitrack Motion Capture system was used in this experiment. For this purpose, motion capture markers were attached to the device. In addition, in this experiment, the scaling parameter in the (9) was set to $\boldsymbol{k}_p = [1.0, 1.0, 1.0]^T$.

The articulated aerial robot used for operation is the HYDRUS_XI proposed by Zhao et al. [7] as shown in the right side of Fig. 6. This robot consists of four links, and each joint has freedom of rotation only in the yaw direction. In addition, since this robot is underactuated, it is possible to operate the positions x, y, z, and rotation in the yaw direction. The Motion Capture system obtains the robot's position and attitude in the same way as the device.

B. Teleoperation Experiment

The operator performed teleoperation using the proposed framework. The appearance of the experiment is shown in Fig. 7, and the operator uses the proposed device with both hands to operate the position, attitude, and joint angles of the articulated aerial robot. The operator directly observes the robot and receives visual feedback. Fig. 8 shows a plot comparing the command values during operation and the actual measured values. The position and attitude are measured by the Motion Capture system, and the joint angles are measured by the servo motors of the robot joints. The RMSE and delay time for each are shown in Table. I and Table. II.

Through this experiment, the operator was able to operate all DoF of the robot simultaneously without confusion. On the other hand, there was a delay of more than one second in the x, y, and yaw directions, which made the operator feel uneasy during operation. This is thought to be due to the controller of the robot used in this experiment. The robot used a PID controller to change the propeller speed to achieve the target position and attitude. Since the tracking performance can be changed by the PID gain, it is thought that the trackability can be improved by using other controllers, such as a properly tuned PID controller or MPC method.

In addition, when the operator attempted to move the position, attitude, or joint angles independently, other operation commands were unintentionally generated. As discussed in Sec. II, it is theoretically possible to operate each independently by using both hands. However, it is difficult for humans to achieve the constraint of not moving factors other than those they want to operate without any assistance. One method to make this possible is to present a reaction force or torque based on resilience or hysteresis when attempting to move the position, attitude, or joint angles.

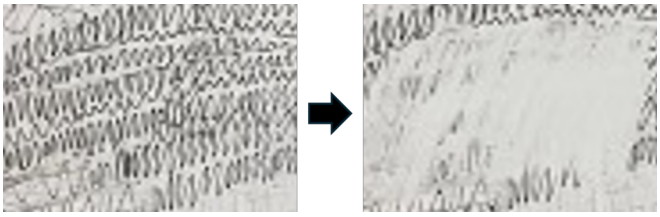

Fig. 9: The result of the wall cleaning experiment. Left: Snapshot of the ink on the whiteboard before cleaning. Right: After cleaning.

C. Wall Cleaning Experiment

Next, we conducted a challenging experiment involving aerial manipulation by teleoperation of an articulated aerial robot. In this experiment, we simulated cleaning the walls of a high-rise building by wiping ink off a whiteboard. We attached a cleaning end effector to the end of the link of the articulated aerial robot HYDRUS_XI. Fig. 1 shows the appearance of the experiment. As shown in Figure 9, the operator succeeded to wipe off the ink by teleoperation.

However, it was unable to wipe off all of the ink completely. In order to wipe completely, it is important to press the cleaning tool onto the surface. However, in our proposed system, it was difficult for the operator to recognize the force applied to the robot's end effector, and it was not possible to press the end effector sufficiently onto the surface. In addition, friction between the wall surface and the end effector caused the robot to rotate in an unintended direction. This made it more difficult to press the cleaning tool onto the wall surface. When performing tasks that involve contact with the environment, it is necessary to provide feedback that allows the operator to correctly recognize the external forces exerted on the robot by the environment. With appropriate feedback functions, the operator can make the correct judgment depending on the situation and perform the task more intuitively.

Furthermore, when performing such long-duration tasks, the device's floating base characteristic may increase operator fatigue. This is because even simple maneuvers that do not involve joint manipulation always require operation with both hands. While this research aimed to control all DoF of the robot simultaneously with both hands, there is a possibility that hybrid use with conventional joystick-type control methods is effective when considering operator fatigue.

V. CONCLUSION

In this study, we proposed a framework that enables the intuitive teleoperation of multiple DoF of a robot simultaneously in order to expand the freedom of operation

by using an articulated aerial robot for high-altitude work. The framework consists of a floating-based device that can operate all DoF of the articulated aerial robot with both hands, and a system that converts the DoF of the operator's hands into commands to the robot. The effectiveness of the proposed framework was demonstrated through teleoperation experiments using a real robot. The experiments conducted in this study were limited to simple indoor tests. However we will conduct outdoor experiments closer to real-world conditions in the future. We believe that the proposed method, which can control all joints of the articulated aerial robot, will enable more efficient wall cleaning than conventional methods on outdoor walls with obstacles.

As future work, we aim to integrate information feedback from the robot to the operator to make the system bilateral. Haptic feedback is considered essential, especially in the execution of tasks involving contact with the environment, as attempted in this study. The integration of haptic feedback is expected to enable teleoperation in environments with limited visibility.

Research on haptic feedback for teleoperation of aerial robots is progressing, and there are systems that use vibration, such as [16], and systems that present reaction forces to the operator's hands, such as [17]. However, both are limited to cases in which the robot can be treated as a single rigid body, and cannot be used as is when operating an articulated aerial robot. In the future, we aim to develop a system that provides haptic feedback of the forces exerted on the end effector of an articulated aerial robots.

REFERENCES

[1] T. Wang, K. Umemoto, T. Endo, and F. Matsuno, "Modeling and control of a quadrotor uav equipped with a flexible arm in vertical plane," *IEEE Access*, vol. 9, pp. 98 476–98 489, 2021.

[2] S. M. Uddin, M. R. Hossain, M. S. Rabbi, M. A. Hasan, and M. S. Rahman Zishan, "Unmanned aerial vehicle for cleaning the high rise buildings," in *2019 International Conference on Robotics,Electrical and Signal Processing Techniques (ICREST)*, 2019, pp. 657–661.

[3] X. Meng, Y. He, Q. Wang, T. Yan, and J. Han, "Force-sensorless contact force control of an aerial manipulator system," in *2018 IEEE International Conference on Real-time Computing and Robotics (RCAR)*, 2018, pp. 595–600.

[4] M. Ryll, H. H. Bülthoff, and P. R. Giordano, "A novel overactuated quadrotor unmanned aerial vehicle: Modeling, control, and experimental validation," *IEEE Transactions on Control Systems Technology*, vol. 23, no. 2, pp. 540–556, 2015.

[5] S. Park, J. Her, J. Kim, and D. Lee, "Design, modeling and control of omni-directional aerial robot," in *2016 IEEE/RSJ International Conference on Intelligent Robots and Systems (IROS)*, 2016, pp. 1570–1575.

[6] M. Kamel, S. Verling, O. Elkhatib, C. Sprecher, P. Wulkop, Z. Taylor, R. Siegwart, and I. Gilitschenski, "The voliro omniorientational hexacopter: An agile and maneuverable tiltable-rotor aerial vehicle," *IEEE Robotics & Automation Magazine*, vol. 25, no. 4, pp. 34–44, 2018.

[7] M. Zhao, T. Anzai, K. Okada, K. Kawasaki, and M. Inaba, "Singularity-free aerial deformation by two-dimensional multilinked aerial robot with 1-dof vectorable propeller," *IEEE Robotics and Automation Letters*, vol. 6, no. 2, pp. 1367–1374, 2021.

[8] M. Zhao, T. Anzai, F. Shi, X. Chen, K. Okada, and M. Inaba, "Design, modeling, and control of an aerial robot dragon: A dual-rotor-embedded multilink robot with the ability of multi-degree-of-freedom aerial transformation," *IEEE Robotics and Automation Letters*, vol. 3, no. 2, pp. 1176–1183, 2018.

[9] H. Yang, S. Park, J. Lee, J. Ahn, D. Son, and D. Lee, "Lasdra: Large-size aerial skeleton system with distributed rotor actuation," in *2018 IEEE International Conference on Robotics and Automation (ICRA)*, 2018, pp. 7017–7023.

[10] L. Shi, N. J. H. Marcano, and R. H. Jacobsen, "A survey on multi-unmanned aerial vehicle communications for autonomous inspections," in *2019 22nd Euromicro Conference on Digital System Design (DSD)*, 2019, pp. 580–587.

[11] K. Darvish, L. Penco, J. Ramos, R. Cisneros, J. Pratt, E. Yoshida, S. Ivaldi, and D. Pucci, "Teleoperation of humanoid robots: A survey," *IEEE Transactions on Robotics*, vol. 39, no. 3, pp. 1706–1727, 2023.

[12] A. Nourmohammadi, M. Jafari, and T. O. Zander, "A survey on unmanned aerial vehicle remote control using brain-computer interface," *IEEE Transactions on Human-Machine Systems*, vol. 48, no. 4, pp. 337–348, 2018.

[13] M. Aggravi, C. Pacchierotti, and P. R. Giordano, "Connectivity-maintenance teleoperation of a uav fleet with wearable haptic feedback," *IEEE Transactions on Automation Science and Engineering*, vol. 18, no. 3, pp. 1243–1262, 2021.

[14] G. A. Yashin, D. Trinitatova, R. T. Agishev, R. Ibrahimov, and D. Tsetserukou, "Aerovr: Virtual reality-based teleoperation with tactile feedback for aerial manipulation," in *2019 19th International Conference on Advanced Robotics (ICAR)*, 2019, pp. 767–772.

[15] D. Kim and P. Y. Oh, "Testing-and-evaluation platform for haptics-based aerial manipulation with drones," in *2020 American Control Conference (ACC)*, 2020, pp. 1453–1458.

[16] M. Macchini, T. Havy, A. Weber, F. Schiano, and D. Floreano, "Hand-worn haptic interface for drone teleoperation," in *2020 IEEE International Conference on Robotics and Automation (ICRA)*, 2020, pp. 10 212–10 218.

[17] M. Allenspach, N. Lawrance, M. Tognon, and R. Siegwart, "Towards 6dof bilateral teleoperation of an omnidirectional aerial vehicle for aerial physical interaction," in *2022 International Conference on Robotics and Automation (ICRA)*, 2022, pp. 9302–9308.